© 2019. Published by The Company of Biologists Ltd | Journal of Cell Science (2019) 132, jcs232249. doi:10.1242/jcs.232249

TOOLS AND RESOURCES

Proximity-dependent biotinylation mediated by TurboID to identify protein–protein interaction networks in yeast

Marc Larochelle, Danny Bergeron, Bruno Arcand and François Bachand*

ABSTRACT

The use of proximity-dependent biotinylation assays coupled to mass spectrometry (PDB-MS) has changed the field of protein–protein interaction studies. However, despite the recurrent and successful use of BioID-based protein–protein interactions screening in mammalian cells, the implementation of PDB-MS in yeast has not been effective. Here, we report a simple and rapid approach in yeast to effectively screen for proximal and interacting proteins in their natural cellular environment by using TurboID, a recently described version of the BirA biotin ligase. Using the protein arginine methyltransferase Rmt3 and the RNA exosome subunits, Rrp6 and Dis3, the application of PDB-MS in yeast by using TurboID was able to recover protein–protein interactions previously identified using other biochemical approaches and provided new complementary information for a given protein bait. The development of a rapid and effective PDB assay that can systematically analyze protein–protein interactions in living yeast cells opens the way for large-scale proteomics studies in this powerful model organism.

KEY WORDS: Proximal biotinylation, TurboID, Yeast, Protein–protein interactions, RNA exosome

INTRODUCTION

Protein–protein interactions, either transient or as part of stable complexes, are key to most cellular processes and biological pathways. In recent years, it has in fact become clear that a detailed description of specific protein interaction networks is required for our understanding of many disease states and the development of new drugs (Goodacre et al., 2018; Laddach et al., 2018). Accordingly, experimental approaches dedicated to the identification of protein–protein interactions are fundamental to understanding complex biological processes. Affinity purification coupled to mass spectrometry (AP-MS) has been an invaluable technique for identifying interaction partners in many experimental systems, including yeast, *Drosophila*, plants and humans (Dunham et al., 2012). However, there are limitations to the successful identification of interaction partners by AP-MS. First, AP-MS is largely dependent on the rate of dissociation of protein–protein interactions or of a protein complex (Lambert et al., 2015), thereby limiting the identification of transient or weak interactions. In addition, complex insolubility, common for chromatin- and membrane-associated proteins, is another limitation associated with AP-MS.

RNA Group, Department of Biochemistry, Université de Sherbrooke, Sherbrooke, QC, J1E 4K8 Canada.

*Author for correspondence (f.bachand@usherbrooke.ca)

F.B., 0000-0002-3661-9767

Received 25 March 2019; Accepted 29 April 2019

An alternative approach to AP-MS was described by Roux and colleagues (Roux et al., 2012) and relies on proximity-dependent biotinylation (PDB) via a modified version of an *E. coli* biotin ligase (BirA) that is fused in frame to a protein of interest, an assay that was termed BioID. This mutant version of BirA uses biotin to catalyze the formation of biotinoyl-5′-AMP (bioAMP), thereby generating a ‘cloud’ of activated biotin molecules that can react with free primary amines (most often lysine residues) of neighboring proteins (see Fig. 1A), thus allowing biotinylation of proximal proteins in the native cellular environment. Since interaction partners and proximal proteins are covalently marked with biotin groups, they can be subsequently captured via a streptavidin-based affinity purification procedure and identified by mass spectrometry. Notably, because of the high affinity of the streptavidin–biotin bond, BioID assays are usually performed under stringent denaturing conditions, which effectively solubilize most cellular proteins as well as reducing nonspecific binding and post-lysis reassortments of protein complexes. More recently, newer versions of the BirA biotin ligase have been developed that enable more-selective targeting of fusion proteins, require less biotin supplementation to the culture media, and exhibit enhanced labeling kinetics for adjacent proteins (Branon et al., 2018; Kim et al., 2016). Notably, the recent development of TurboID, which can catalyze protein biotinylation on a timescale of minutes instead of several hours for BioID and BioID2, may allow PDB assays to be used to study dynamic protein–protein interactions.

The yeasts *Saccharomyces cerevisiae* and *Schizosaccharomyces pombe* are two unicellular organisms that are used as model systems by thousands of laboratories around the world for studies related to gene regulation, the cell cycle, chromosome dynamics, epigenetics, DNA repair and several other evolutionarily conserved cellular processes (Amberg and Burke, 2016; Hoffman et al., 2015). Furthermore, yeast has been a valuable eukaryotic model system, not only for traditional molecular and cell biology, but also for the fields of functional genomics and proteomics. Although AP-MS approaches, most notably tandem affinity purifications (TAP), have been extensively used in both *S. cerevisiae* (Rigaut et al., 1999) and *S. pombe* (Tasto et al., 2001) for the identification of protein–protein interactions, the use of PDB in yeast has been minimal when compared to its frequent application in mammalian cells. One of the potential reasons for the limited use of PDB in yeast is the fact that the BioID- and BioID2-based biotin ligases are most active at 37°C, which is the optimal temperature of *E. coli* BirA. However, a growth temperature of 37°C induces strong stress responses in both *S. cerevisiae* (Causton et al., 2001; Gasch et al., 2000) and *S. pombe* (Chen et al., 2003), which is optimally grown at lower temperatures (30°C). Interestingly, as the TurboID version of BirA was molecularly evolved in a yeast system, TurboID exhibits high PDB activity at 30°C (Branon et al., 2018).

An analogous proximal protein biotinylation assay based on a genetically engineered ascorbate peroxidase (APEX2) was previously adapted to yeast cells (Hwang and Espenshade, 2016).

Journal of Cell Science (2019) 132, jcs232249. doi:10.1242/jcs.232249

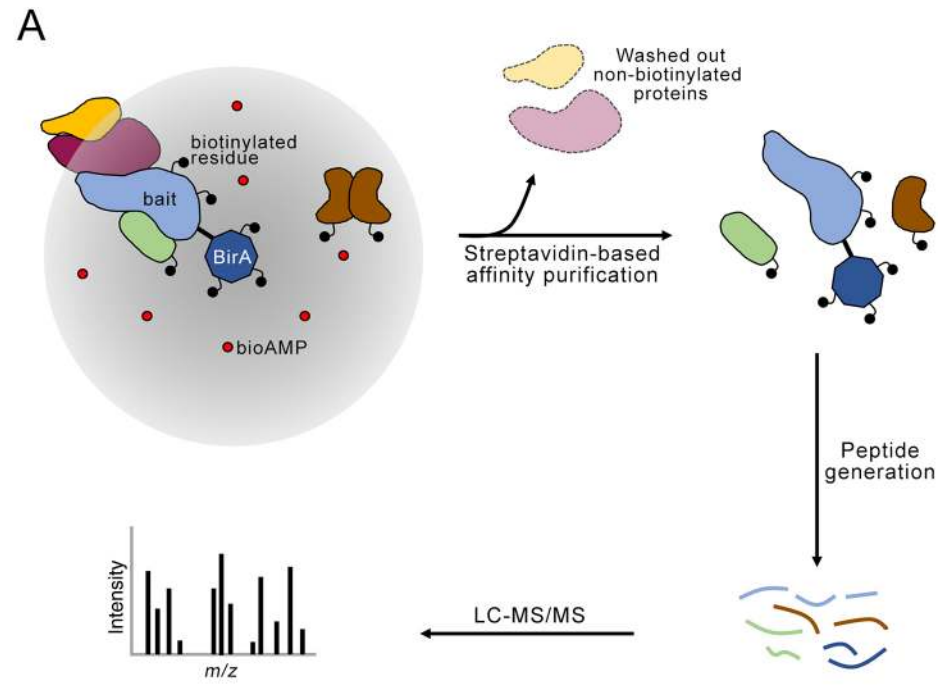

Fig. 1. Use of PDB to screen for proximal protein–protein interactions. (A) In PDB, a modified version of *E. coli* BirA is fused in frame to a protein of interest (bait) that is expressed in its natural context. BirA will use biotin to catalyze the formation of activated biotin (bioAMP, red circles), which can react with lysine residues of adjacent proteins to create covalent biotin tags (black circles). Cell lysis and affinity purification of biotinylated proteins using streptavidin-coated beads is followed by peptide generation by proteolysis (e.g. trypsin). Peptides are subsequently analyzed by LC-MS/MS for protein identification. (B) Schematic representation of the structure of the pFA6a-based vectors for C-terminal tagging of genes with TurboID-3×Myc. These vectors allow the expression of a gene of interest from the native promoter at the endogenous locus in *S. cerevisiae* and *S. pombe* by providing resistance to either geneticin (kan^R) or nourseothricin (nat^R). Primers for the one-step PCR method are shown as arrows outside the boxes (not to scale).

However, as APEX-based protein biotinylation requires biotin-phenol as a substrate (instead of biotin for BioID and TurboID) and necessitates the addition of hydrogen peroxide for peroxidase activation, additional steps are required to perform optimal APEX2 labeling in yeast to facilitate biotin-phenol uptake, including high osmolarity and disruption of the cell wall using zymolase (Hung et al., 2016; Hwang and Espenshade, 2016). As hydrogen peroxide is toxic to living cells, and high osmolarity induces a strong stress response, new and better tools are therefore needed to use PDB-MS to study protein–protein interaction network in yeast.

The development of a modified version of BirA (TurboID) that exhibits greater efficiency than BioID and BioID2 and displays high activity at 30°C led us to investigate how generally applicable PDB using TurboID could be in yeast. Here, we have adapted the TurboID system for use in the fission yeast *S. pombe*, and report the construction of pFA6-based vectors for this purpose. These vectors utilize the *kanMX* and *natMX* cassettes, which allow for positive selection of integration in either *S. pombe* or *S. cerevisiae*, and avoid the need for a specific auxotrophic background (Bähler et al., 1998; Longtine et al., 1998). To demonstrate the functionality of TurboID in yeast, we tested whether we could identify known protein interaction partners of the protein arginine methyltransferase Rmt3, as well as the RNA exosome-associated exonucleases Dis3 and Rrp6. Rmt3 is a cytosolic protein that is known to form an extra-ribosomal complex with the 40S ribosomal protein S2, a complex that is conserved from yeast to humans (Bachand and Silver, 2004; Landry-Voyer et al., 2016). On the other hand, the eukaryotic exosome is an RNA degradation complex that adopts a barrel-like structure consisting of two stacked rings with a prominent central channel that is wide enough to accommodate single-stranded (ss)RNA (Liu et al., 2006). The bottom ring is composed of six catalytically inactive RNase PH-like proteins (Rrp41, Rrp42, Rrp43, Rrp45, Rrp46 and Mtr3), while three S1/KH RNA-binding proteins (Rrp4, Rrp40 and Csl4) form the top ring, which is often referred to as the exosome cap structure (Makino et al., 2013). Two additional subunits provide the catalytic activity of the eukaryotic exosome: Rrp6, which is exclusive to the nuclear exosome, exhibits distributive 3′-5′ exonucleolytic activity and is attached to the cap structure, while Dis3 is a processive 3′-5′ exoribonuclease that is anchored to the bottom PH-like ring and is found in both the cytoplasmic and nuclear exosome (Zinder and Lima, 2017). The use of TurboID for PDB in yeast revealed a number of abundant interaction candidates, among which are known interactors of Rmt3, Dis3 and Rrp6. In addition, newly identified interaction candidates fell into functional categories that included transcription, chromatin regulation, and DNA repair. Taken together, our findings demonstrate that TurboID is a relatively simple and rapid technique to effectively screen for proximal and interacting proteins in yeast.

RESULTS

To exploit TurboID in yeast, we generated constructs designed for C-terminal tagging of target proteins at endogenous chromosomal loci. The cDNA coding for the TurboID version of the BirA biotin

Journal of Cell Science (2019) 132, jcs232249. doi:10.1242/jcs.232249

ligase (Branon et al., 2018) was fused to sequences encoding three tandem copies of the Myc epitope (3Myc) and assembled into the pFA6a backbone with either *kanMX6* or *natMX6* markers for selection on geneticin- and nourseothricin-supplemented media, respectively (Fig. 1B). In addition to offering options between selection markers, nourseothricin is effective in both rich and minimal media, whereas geneticin works only in rich media. Accordingly, this construct was designed such that oligonucleotides used to generate gene-specific PCR cassettes for C-terminal tagging with previously described tags in *S. cerevisiae* (Longtine et al., 1998) and *S. pombe* (Bähler et al., 1998) would be compatible with the TurboID tagging constructs.

To demonstrate the feasibility of the TurboID system in yeast, we initially tagged the C-terminal of the protein arginine methyltransferase Rmt3, and of the 3′-5′ exoribonuclease Dis3, with the 35-kDa TurboID biotin ligase in *S. pombe*. Rmt3 and Dis3 were selected because affinity purification-coupled mass spectrometry (AP-MS) approaches previously revealed a set of known Rmt3- and Dis3-associated proteins (Bachand and Silver, 2004; Telekawa et al., 2018). Western blot analysis using anti-Myc antibody confirmed the successful tagging of both Rmt3 and Dis3 (Fig. 2A, lanes 1–3); the tagged proteins displayed molecular masses of ∼100 kDa and ∼150 kDa, respectively, which is roughly 35 kDa greater than the mass of untagged Rmt3 (62 kDa) and Dis3 (110 kDa), and consistent with C-terminal fusions with TurboID (Branon et al., 2018).

Next, we examined for evidence of TurboID-mediated biotinylation in live yeast cells. Tagging of a bait protein with a biotin ligase derivative is known to induce extensive self-biotinylation of the bait protein (Branon et al., 2018; Roux et al., 2012). As the Rmt3-TurboID and Dis3-TurboID strains were grown in biotin-containing rich medium, we thus examined for evidence of Rmt3 and Dis3 biotinylation. Streptavidin blot analysis of a total extract prepared from a control untagged strain detected endogenous biotinylated proteins, including the ∼130-kDa pyruvate carboxylase Pyr1, and the ∼250-kDa acetyl-CoA carboxylase Cut6, which are known to be biotinylated (Tong, 2013) and likely correspond to the stronger signals on the streptavidin blot (Fig. 2A, lane 4, see asterisks). Importantly, streptavidin blot analysis of Rmt3-TurboID and Dis3-TurboID strains revealed new biotinylated proteins at 100 kDa and 150 kDa, respectively (Fig. 2A, lanes 5–6), consistent with self-biotinylation of the Rmt3-TurboID and Dis3-TurboID fusions. Notably, as *dis3* is an essential gene, our results also indicate that the presence of the 35-kDa TurboID tag and the self-biotinylation of Dis3 did not perturb its essential functions, as growth of the Dis3-TurboID strain was comparable to the control untagged strain.

We also confirmed that TurboID-dependent biotinylated proteins could be affinity purified using streptavidin-coated beads. As shown in Fig. 2B, Rmt3-tagged TurboID was specifically recovered in the streptavidin pulldown (see lane 7), whereas no signal was detected using extracts prepared from the control untagged strain (lane 6). Notably, efficient capture of biotin-tagged Rmt3 was demonstrated by the substantial depletion of Rmt3-TurboID from the starting extract (compare lane 4 to lane 2), whereas non-biotinylated Rmt3 was not depleted from the total extract (compare lane 3 to lane 1). Taken together, these results indicate efficient proximity biotin labeling with TurboID in living yeast cells.

Protocols for proximity-dependent biotinylation using BioID and BioID2 rely on the addition of exogenous biotin to the culture medium for several hours to induce BirA-mediated biotinylation of adjacent proteins (Kim et al., 2016; Roux et al., 2012). In contrast, as the TurboID version of BirA exhibits greater catalytic activity compared to BioID and BioID2 (Branon et al., 2018), protein biotinylation was observed before the addition of exogenous biotin when using TurboID in yeast. Specifically, our initial tests for Rmt3 and Dis3 self-biotinylation (Fig. 2A) in *S. pombe* were performed in rich culture medium (YES) without addition of exogenous biotin, indicating that the Rmt3-TurboID and Dis3-TurboID fusions can utilize the physiological levels of biotin present in yeast cells that are grown in biotin-containing rich media. To test whether addition of exogenous biotin to growing yeast cells would induce increased levels of protein biotinylation, we analyzed self-biotinylation of TurboID-tagged Rmt3 from cells grown in rich and minimal media

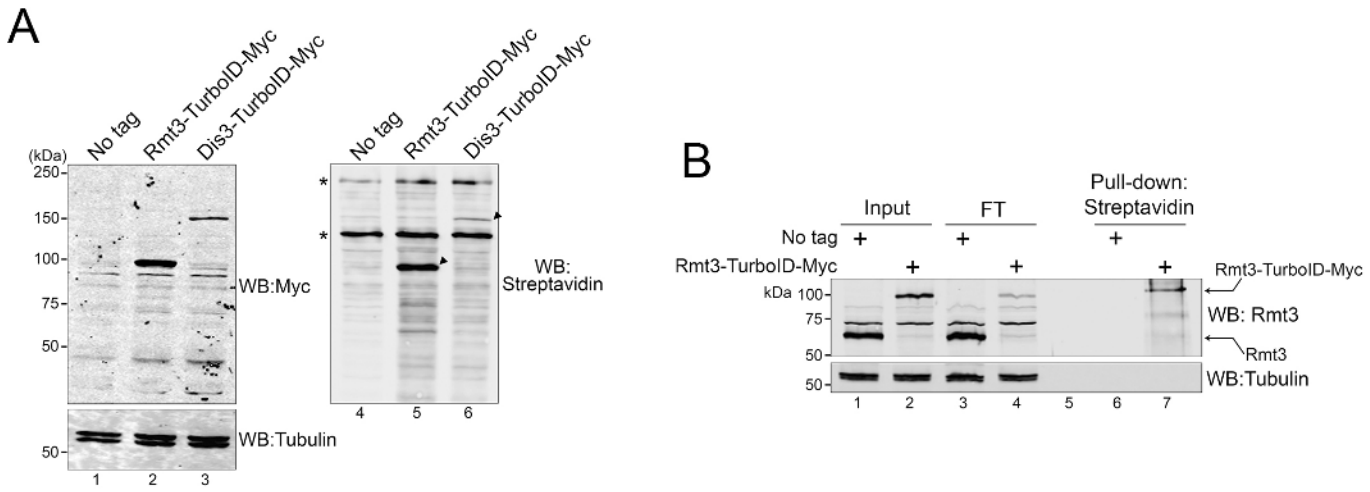

Fig. 2. Proximal biotinylation of Rmt3 and Dis3 in fission yeast by TurboID. (A) Western blot analysis of total cell extracts prepared from a control untagged strain (lanes 1 and 4) as well as strains that express TurboID-3×Myc-tagged versions of Rmt3 (lanes 2 and 5) and Dis3 (lanes 3 and 6). Western blot (WB) analysis was performed using anti-Myc and anti-tubulin (left) antibodies and IRDye-coupled streptavidin (right). Asterisks (right panel) indicate the position of the 130-kDa pyruvate carboxylase (Pyr1) and the 250-kDa acetyl-CoA carboxylase (Cut6), which are endogenously biotinylated proteins. Arrowheads show auto-biotinylation of Rmt3 (lane 5) and Dis3 (lane 6). (B) Western blot analysis of total cell extracts (lanes 1 and 2), flow-through (FT) fractions (lanes 3 and 4), and streptavidin pulldown (lanes 6 and 7) prepared from control untagged (lanes 1, 3, and 6) and Rmt3-TurboID-3×Myc (lanes 2, 4 and 7) strains. Western blot analysis was performed using anti-Rmt3 (top) and anti-tubulin (bottom) antibodies. The positions of untagged Rmt3 and Rmt3-TurboID-3×Myc are indicated on the right.

Journal of Cell Science (2019) 132, jcs232249. doi:10.1242/jcs.232249

after addition of exogenous biotin. As shown in Fig. 3A, addition of exogenous biotin to both rich and minimal media did not result in increased levels of Rmt3 self-biotinylation (compare lane 4 to lane 3 and lane 8 to lane 7). These data indicate that both rich and minimal media provide a sufficiently high intracellular concentration of biotin to support proximity-dependent biotinylation from the TurboID version of BirA in fission yeast. We thus conclude that the addition of exogenous biotin is not required for proximity-dependent biotinylation of Rmt3 using TurboID in *S. pombe*. However, it is likely that Rmt3 is near saturation levels in terms of protein biotinylation due to its close proximity to the TurboID biotin ligase. Accordingly, we cannot exclude the possibility that addition of exogenous biotin may be beneficial for the identification of transient protein–protein interactions using TurboID in yeast.

Although *S. pombe* is auxotrophic for biotin, as it is unable to synthesize biotin *de novo*, a biotin transporter allows uptake of biotin in fission yeast (Stolz, 2003). Since we could not activate TurboID in fission yeast by adding exogenous biotin to the culture media (Fig. 3A), we tested whether addition of exogenous biotin to cells that were previously incubated in a biotin-free medium would result in a temporal activation of TurboID-dependent biotinylation. An exponentially growing culture of Rmt3-TurboID cells grown in minimal EMM (containing biotin) was used to inoculate fresh biotin-free EMM at a starting optical density at 600 nm (OD_{600}) of 0.015. After overnight incubation at 30°C, exogenous biotin was added to a final concentration of 50 µM and samples were harvested at different time points for analysis of Rmt3 self-biotinylation. Notably, growth of the Rmt3-TurboID strain in biotin-free medium resulted in a significant reduction of Rmt3 biotinylation as compared to the same strain grown in biotin-supplemented medium (Fig. 3B, compare lanes 2 and 3). Importantly, Rmt3 biotinylation was clearly detected 30 min after the addition of exogenous biotin and steadily increased to reach steady state levels at 3 h (Fig. 3B, lanes 4–8). Collectively, these data indicate that proximity-dependent biotinylation in yeast using TurboID is robust and effective using biotin concentrations present in yeast media. Alternatively, addition of exogenous biotin to biotin-free media for a labeling time of 1–3 h produces sufficient biotinylated proteins for analysis.

Next, we set out to test PDB assays using our strains that express TurboID-tagged Rmt3 and Dis3. In addition, we analyzed a second subunit of the RNA exosome complex, Rrp6, which is localized exclusively to the nucleus in yeast, whereas Dis3 is found in both the nucleus and the cytoplasm (Allmang et al., 1999). In contrast, Rmt3 is exclusively cytoplasmic (Bachand and Silver, 2004). As a control, cells from an untagged strain were processed in parallel. For these experiments, 50 ml of yeast cultures with an OD_{600} value ∼0.6 were lyzed under stringent denaturing conditions using SDS-containing buffer. Biotinylated proteins were then captured with streptavidin-coated beads, which were washed rigorously and subjected to on-bead trypsin digestion to release peptides for analysis by MS. Based on two independent biological replicates, we reproducibly identified 19, 299, 125 and 131 proteins with a sequence coverage ≥10% and a minimum of three detectable peptides in the untagged, Rmt3-TurboID, Rrp6-TurboID and Dis3-TurboID strains, respectively (Tables S2–S5). As expected, the strongly biotinylated Pyr1 and Cut6 proteins were consistently identified as the top hits in all four strains (Tables S2–S5). Such endogenously biotinylated proteins were filtered out (Filter 1) from our lists of biotinylated proteins by excluding proteins that were detected in streptavidin pulldowns prepared from the control untagged strain. Moreover, given the different localization of Rmt3 (exclusively cytosolic), Dis3 (nuclear and cytosolic), and Rrp6 (exclusively nuclear), we reasoned that biotinylated proteins that were common to Rmt3, Dis3 and Rrp6 were unlikely to be specific interacting proteins. We therefore removed 47 biotinylated proteins (Filter 2; Table S6) that were identified in TurboID assays from all three strains that expressed a TurboID-tagged protein. Thus, after filtering, 217, 43 and 44 TurboID-based interactions were assigned to Rmt3, Rrp6 and Dis3, respectively (Tables S7–S9).

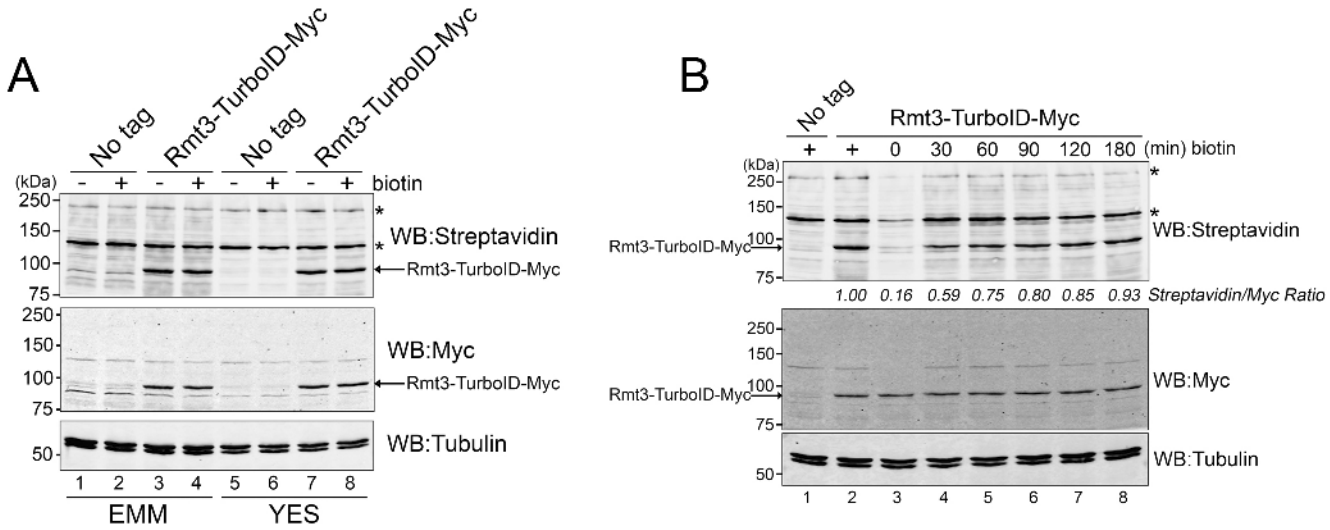

Fig. 3. Addition of exogenous biotin is not required for Rmt3 self-biotinylation by TurboID. (A) Western blot (WB) analysis of total extracts prepared from a control untagged strain (lanes 1, 2, 5 and 6) and the Rmt3-TurboID-3Myc strain (lanes 3, 4, 7 and 8). Cells were cultured in minimal (EMM, lanes 1–4) or rich (YES, lanes 5–8) media in the absence (lanes 1, 3, 5 and 7) or presence (lanes 2, 4, 6 and 8) of 50 µM of exogenous biotin. Western blot analysis was performed using anti-Myc (middle) and anti-tubulin (bottom) antibodies and IRDye-coupled streptavidin (top). Asterisks indicate the positions of the 130-kDa Pyr1 and 250-kDa Cut6 proteins, which are endogenously biotinylated proteins. (B) Western blot analysis of total extracts prepared from a control untagged strain (lane 1) and the Rmt3-TurboID-3×Myc strain (lanes 2–8). Cells were cultured in normal EMM (lanes 1 and 2) or grown in biotin-free EMM (lane 3), which was supplemented with 50 µM of exogenous biotin for the indicated times (lanes 4–8). Western blot analysis was performed as in A.

Journal of Cell Science (2019) 132, jcs232249. doi:10.1242/jcs.232249

To assess the relative abundance of the identified proteins for the individual TurboID assays, we used a label-free intensity-based quantification approach (Schwanhäusser et al., 2011) that calculates the sum of all peptide peak intensities matching to a specific protein. Fig. 4A–C shows such relative peptide intensity analyses plotted against the protein sequence coverage (percentage of amino acid of a protein identified by MS). Notably, our TurboID analysis of Rmt3 disclosed the 40S ribosomal protein uS5 (Rps2) as a top hit (Fig. 4A), consistent with previous AP-MS analyses of *S. pombe* Rmt3 (Bachand and Silver, 2004) and human PRMT3 (Landry-Voyer et al., 2016), denoting the existence of an evolutionarily conserved extra-ribosomal complex between Rps2 and Rmt3. In contrast, Rps2 was not detected in TurboID assays of Dis3 and Rrp6. In addition to Rps2, our TurboID analysis of Rmt3 identified over 200 proteins, including the *S. pombe* homologs of human PDCD2, Trs401 and Trs402 (Fig. 4A), which were not identified in a previous AP-MS analysis of Rmt3-associated proteins (Bachand and Silver, 2004). The identification of Trs401 and Trs402 in the TurboID analysis of Rmt3 is significant, as co-purification of PDCD2 and PRMT3 was reported in human cells (Landry-Voyer et al., 2016), which also supports evolutionarily conserved interactions. A gene ontology (GO) enrichment analysis (Berriz et al., 2003) for proteins identified in the TurboID assay of Rmt3 revealed attributes related to cytosolic components and several metabolic processes, as well as aminoacyl-tRNA ligase activity. As expected for Dis3 and Rrp6, GO analyses revealed significant enrichments for functions related to the RNA exosome, rRNA processing, nuclear RNA surveillance, nuclear polyadenylation-dependent non-coding (nc)RNA catabolic process, the Mmi1 nuclear focus complex and the TRAMP complex. Accordingly, many proteins that were previously shown to be associated with the RNA exosome by AP-MS were found to be biotinylated in our TurboID assays of Dis3 and Rrp6 (Fig. 4B,C), including the components of the TRAMP complex Mtr4 and Cid14, the nuclear exosome-associated protein Mpp6, and components of the MTREC/NURS complex, namely Mmi1, Cti1, Iss10, and Mtl1 (Egan et al., 2014; Lee et al., 2013; Telekawa et al., 2018; Zhou et al., 2015).

Interestingly, analysis of the different proteins identified in our independent TurboID assays revealed a significant overlap in the set of biotinylated proteins identified between Rmt3 and Dis3 (Fig. 4D, 1.4×10^{-11}, Fisher's exact test) as well as between Dis3 and Rrp6 (Fig. 4D, 7.4×10^{-30}, Fisher's exact test). Whereas biotinylated proteins overlapping between TurboID assays of Dis3 and Rrp6 (n=19; Table S10) are expected to be relevant to the related functions of these proteins in RNA processing, the set of overlapping proteins biotinylated in TurboID assays of Rmt3 and Dis3 (n=16, Table S11) are likely to represent nonspecific candidates resulting from the presence of these two proteins in the cytoplasm. Accordingly, no overlap was found between Rmt3 and Rrp6, which localize to different subcellular compartment, namely the cytosol and the nucleus, respectively. Furthermore, the proteins

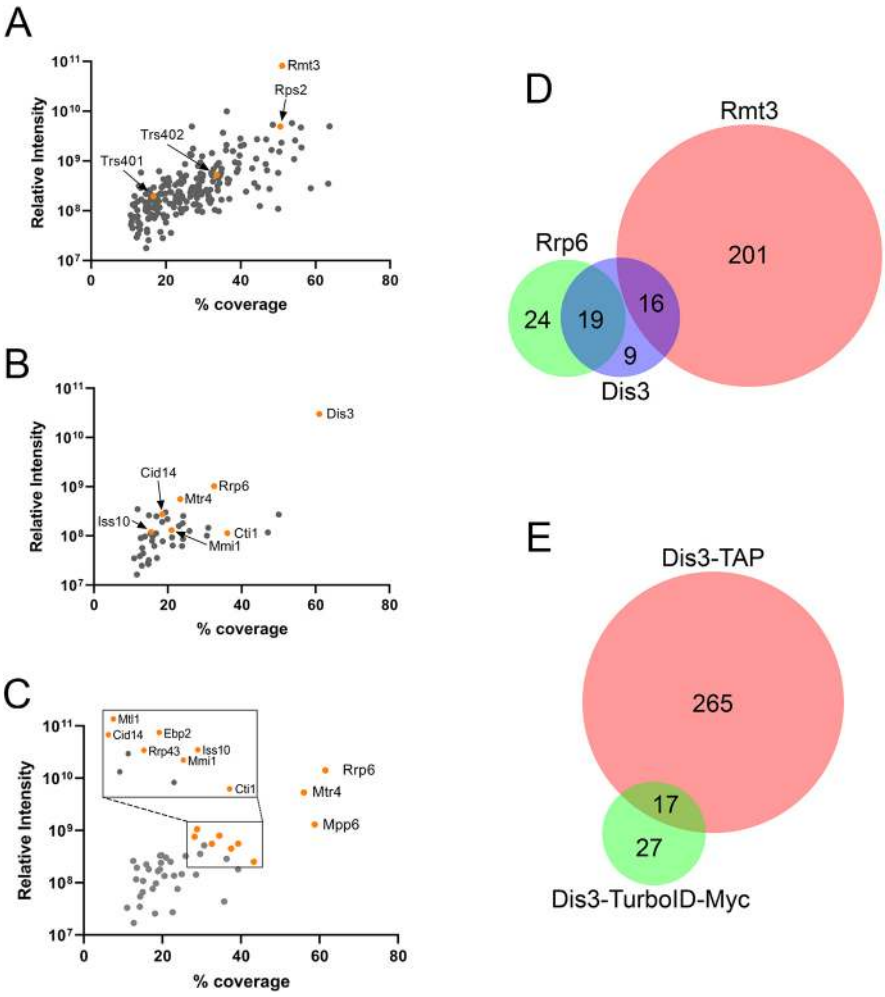

Fig. 4. PDB-MS of Rmt3, Dis3 and Rrp6 in yeast cells. (A–C) Scatter plots of PDB-MS assays after streptavidin-based purification of biotinylated proteins from extracts of cells expressing TurboID-tagged Rmt3 (A), Dis3 (B), and Rrp6 (C) as plotted by protein abundance (relative peptide intensity) up the *y*-axis and percentage sequence coverage (amino acids) on the *x*-axis. Points corresponding to previously established Rmt3-, Dis3-, and Rrp6-interacting proteins are labeled in orange. Results in A–C represent the average from two independent replicate experiments. (D) Venn diagram showing overlap between datasets, after application of Filters 1 and 2 (see text for details). (E) Venn diagram showing overlap between protein–protein interaction identification for *S. pombe* Dis3 by PDB-MS (this study) and AP-MS (Telekawa et al., 2018).

that overlapped between TurboID assays of Rmt3 and Dis3 are amongst the most abundant proteins in the fission yeast proteome (Fig. S1), which is known to increase the propensity of a protein to be a contaminant using approaches that aim to identify protein–protein interactions (Mellacheruvu et al., 2013). We therefore suspect that the 16 proteins biotinylated by both Rmt3-TurboID and Dis3-TurboID fusions are false positives that are caused by the nature of the labeling procedure, protein abundance and the overlapping localization of the bait proteins.

PDB assays and AP-MS are known to be complementary proteomics approaches that can identify different sets of interactions for the same bait protein (Lambert et al., 2015). Recently, we used AP-MS to identify and characterize post-translational modifications in the *S. pombe* RNA exosome complex (Telekawa et al., 2018). In total, 282 proteins were identified in the AP-MS analysis of TAP-tagged Dis3, whereas TurboID assays with Dis3 identified 44 proteins. Significantly, 17 proteins (Table S12) were identified in both approaches (Fig. 4E, $P<6.963\times10^{-11}$, Fisher's exact test), including Rrp6, Mtr4, Cid14, Mmi1, Iss10 and Cti1. Thus, the establishment of the TurboID assay in yeast was able to recapitulate a fraction of protein–protein interactions previously identified using other biochemical approaches and provided new complementary information for a given protein bait. Intriguingly, the TurboID analyzes of Rrp6 and Dis3 were ineffective at identifying core subunits of the RNA exosome. Specifically, only Rrp43 was recovered in the TurboID assay of Rrp6, while TurboID assays of Dis3 did not retrieve any of the ten core exosome subunits. This contrasts to our previous AP-MS analysis of Dis3, as these experiments identified all ten subunits of the core exosome (Telekawa et al., 2018). It is unclear at this point why only a single core subunit of the stable and stoichiometric exosome complex was biotinylated by Rrp6 and Dis3 TurboID fusion proteins. As Dis3 and Rrp6 exonucleases are located at the bottom and top, respectively, of the 11-subunit exosome complex, it is possible that the estimated 10-nm labeling radius of BirA-like biotin ligases in the context of Rrp6 and Dis3 C-terminal fusions may not effectively reach protein subunits that are part of the trimeric cap and inner ring of the RNA exosome. Future PDB assays with core exosome subunits as protein baits should provide additional insights into the ability to identify core subunits of the exosome complex using TurboID.

DISCUSSION

Despite the many advantages that PDB-MS offers over AP-MS, PDB-MS remains an approach that screens for protein–protein interactions, and like most screening methods, it is important to realize that not all of the identified hits will be true proximity partners for the bait of interest. For instance, many hits represent endogenously biotinylated proteins or proteins that are promiscuously biotinylated with most baits. For these reasons, we would like to offer some general advice to users of PDB-MS in yeast. First, one control should minimally include a condition to remove endogenously biotinylated proteins, such an untagged control strain. Second, based on our own experience using BioID in mammalian cells, we prefer to not use a control that mimics promiscuous biotinylation by expression of the BirA biotin ligase alone (BioID or TurboID), as these conditions potentially remove relevant and genuine hits identified with your bait protein. To obtain a more realistic estimation of background, we recommend using a control TurboID fusion that is expressed at levels similar to the bait and shows comparable subcellular localization. Finally, as with most screens for protein–protein interactions, we recommend performing multiple biological replicates of bait and control experiments to confirm the identification of a robust and reproducible set of proximity partners.

In summary, we report the application of a simple and effective PDB assay in yeast using the recently described TurboID protein (Branon et al., 2018). Our work reveals that TurboID-based PDB can be easily coupled to mass spectrometry for large-scale protein–protein interaction screens, as shown for Rmt3, and the RNA exosome subunits, Rrp6 and Dis3. The use of PDB-MS in yeast will therefore allow a comprehensive understanding of spatial and temporal protein–protein interaction networks that can be paired with existing AP-MS datasets to study evolutionarily conserved cellular pathways in this powerful model organism.

MATERIALS AND METHODS

Yeast strains and media

A list of all *S. pombe* strains used in this study is provided in Table S1. Fission yeast cells were routinely grown at 30°C in Edinburg minimal media (EMM2, US biological; E2205) or in yeast extract medium (YES) supplemented with adenine, uracil, leucine and histidine. For liquid chromatography tandem MS (LC-MS/MS) analysis, yeast strains were grown in YES medium supplemented with amino acids, and biotin (Sigma-Aldrich; B4501) was added to a final concentration of 50 µM for 8 h. EMM without biotin (EMM−Biotin, 2030-100) was purchased from Sunrise Science. C-terminal tagging of proteins with TurboID-3×Myc was performed by PCR-mediated gene targeting (Bähler et al., 1998) using the lithium acetate method for yeast transformation. Tagging of proteins was confirmed by western blotting.

TurboID-3×Myc plasmids and amplification module

The TurboID sequence (Branon et al., 2018) containing 3×Myc epitopes was amplified from a DNA G-block using primers FB5858, 5′-CCCCG-GGTTAATTAACATCTTTAAAGACAATACAGTGCCGCTCAAATTG-3′, and FB5859, 5′-GAAGTGGCGCGCCTCACAGATCTTCCTCAGA-GATGAGCTTCTGTTCCAGATC-3′. The PCR insert was digested with *Asc*I-*Pac*I enzymes and inserted into pFA6a-3HA-kanMX6 to replace the DNA sequence encoding the 3HA tag by the DNA sequence encoding TurboID-3×Myc resulting in plasmid pFA6a-TurboID-3Myc-kanMX6 (pFB1420). To create pFA6a-TurboID-3Myc-natMX6 (pFB1434) allowing resistance to nourseothricin, a T_{ADH1}-P_{TEF}-*natMX6*-T_{TEF} DNA fragment obtained from pFA6a-CTAP4-natMX6 (Van Driessche et al., 2005) by *AscI-PmeI* digestion was ligated into *AscI-PmeI*-digested pFB1420 to generate pFB1434. Correct insertions were confirmed by DNA sequencing. Both plasmids can be used as a template to fuse TurboID-3×Myc sequences to the 3′ end of any gene by using PCR primers as follows: forward primer 5′-(gene-specific sequence)-CGGATCCCCGGG-TTAATTAA-3′ and reverse primer 5′-(gene-specific sequence)-GAATTC-GAGCTCGTTTAAAC-3′. The pFA6a-TurboID-3Myc-kanMX6 plasmid was used as a template to fuse the DNA sequence encoding TurboID-3×Myc to the 3′ end of *Rmt3*, *Dis3* and *Rrp6* genes to generate strains FBY2500, FBY2531 and FBY2532, respectively. pFB1420 and pFB1434 are available from Addgene under ID number 126049 and 126050, respectively.

Protein extraction and western blotting

Exponentially growing cells in EMM2 were washed with water and diluted to an $OD_{600\ nm}$ of 0.015 in EMM without biotin for 16 h at 30°C to allow biotin starvation. Following the collection of an initial sample (0-min time point), biotin was added to a final concentration of 50 µM and samples were collected at different time points up to 180 min before protein extraction and western blot analysis. Total cell extracts for protein analyzes by western blotting were prepared as described previously (Lemay et al., 2016). Briefly, cells grown to mid-log phase with or without the presence of biotin were resuspended in ice-cold lysis buffer (50 mM Tris-HCl pH 7.5, 5 mM $MgCl_2$, 150 mM NaCl and 0.1% NP-40) containing 1 mM PMSF, 1× PLAAC and 1× cOmplete protease inhibitor (Millipore Sigma) prior to lysis with glass beads using a Precellys 24 homogenizer system (Bertin

Technologies). Clarified lysates were normalized for total protein concentration by performing a Bradford protein assay. Then, 30 µg of total proteins were separated by SDS-PAGE and transferred to nitrocellulose membranes using a Trans-Blot Turbo System (Bio-Rad). Biotinylated proteins were detected with a Streptavidin Alexa Fluor 680 conjugate [Life Technologies, S21378; 1:20,000 (v/v) dilution] from membranes blocked for 30 min with blocking solution (1% BSA, 0.2% Triton X-100 in PBS) and washed according to Roux et al. (Roux et al., 2018). Immunoblotting was performed as described (Lemay et al., 2014) using a rabbit polyclonal anti-Myc antibody [Santa Cruz Biotechnology, sc-789; 1:500 (v/v) dilution], a mouse monoclonal antibody specific to α-tubulin [Sigma-Aldrich, T5168; 1:1000 (v/v) dilution], and anti-Rmt3 (Perreault et al., 2009) at 1:1000 (v/v) dilution. Membranes were then probed with goat anti-rabbit-IgG or anti-mouse-IgG secondary antibodies conjugated to IRDye 800CW [LI-COR, 926-32213; 1:15,000 (v/v) dilution] and Alexa Fluor 680 [Life Technologies, A-21057; 1:15000 (v/v) dilution], respectively. Protein detection was performed using an Odyssey infrared imaging system (LI-COR).

Affinity capture of biotinylated proteins

Cultures (50 ml) of wild-type (untagged), Rmt3-TurboID-Myc, Dis3-TurboID-Myc, and Rrp6-TurboID-Myc ($OD_{600\ nm}$ of 0.5–0.6) were grown in YES medium supplemented with required amino acids and 50 µM biotin. Cell pellets were resuspended in 250 µl of cold RIPA buffer (50 mM Tris-HCl pH 7.5, 150 mM NaCl, 1.5 mM $MgCl_2$, 1 mM EGTA, 0.1% SDS, 1% NP-40, supplemented with 0.4% sodium deoxycholate, 1 mM DTT, 1 mM PMSF, 1× PLAAC and 1x cOmplete) prior to lysis with glass beads using a Precellys 24 homogenizer system (Bertin Technologies). Sample volume was increased to 500 µl using the same buffer before sonication for three cycles of 10 s at 20% intensity using a Branson Sonifier 250. DNA and RNA were then digested with 250 units of benzonase (Sigma-Aldrich; E1014) for 1 h at 4°C. Clarified lysates were normalized for total protein concentration by performing a Bradford protein assay. Then, 6 mg of total proteins were subjected to affinity purification for 3 h at 4°C with 50 µl of Streptavidin–Sepharose beads (GE Healthcare; 17-5113-01) in 1 ml of cold RIPA buffer containing all supplements with the exception that the SDS concentration was increased from 0.1% to 0.4%. All biotin-based purifications were performed using Protein LoBind tubes (Eppendorf). Beads were then washed once with wash buffer (50 mM Tris-HCl pH 7.5, 2% SDS), three times with RIPA buffer containing DTT (50 mM Tris-HCl pH 7.5, 150 mM NaCl, 1.5 mM $MgCl_2$, 1 mM EGTA, 0.1% SDS, 1% NP-40, 1 mM DTT), and five times with 20 mM ammonium bicarbonate. All washes were done for 5 min at room temperature with agitation. For western blot analysis of streptavidin-bound proteins, biotinylated proteins were eluted from beads for 15 min at room temperature followed by an additional incubation of 15 min at 95°C in SDS-PAGE loading buffer containing 25 mM biotin. For analysis of streptavidin-bound proteins by MS, bound proteins were reduced in 10 mM DTT before being alkylated with 15 mM of iodoacetamide (IAA). Protein-bound beads were subjected to trypsin digestion at 37°C overnight and stopped by the addition of formic acid (final concentration of 1%). Peptides were then extracted using acetonitrile, lyophilized and resuspended in 0.1% trifluoroacetic acid (TFA) to desalt on ZipTips. ZipTips (EMD Millipore) cleanup of peptide samples was performed as described previously (Lemay et al., 2016).

LC-MS/MS analysis

Trypsin-digested samples were analyzed by LC-MS/MS, as described previously (Grenier St-Sauveur et al., 2013; Telekawa et al., 2018). Briefly, following trypsin digestion, peptides were sorted using a Dionex Ultimate 3000 nanoHPLC system. Approximately 2 µg of peptides in 1% (v/v) formic acid was injected with a flow of 4 µl/min on an Acclaim PepMap100 C18 column [0.3 mm internal diameter (i.d.)×5 mm, Dionex Corporation]. Peptides were eluted in a PepMap C18 nanocolumn (75 µm×50 cm, Dionex Corporation) over 240 min with a flow of 200 nl/min using a gradient of 5–35% solvent B (90% acetonitrile with 0.1% formic acid). Through an EasySpray source, the HPLC system was combined to an OrbiTrap QExactive mass spectrometer (Thermo Fisher Scientific). The spray voltage was set to 2.0 kV and the column temperature was set to 40°C. With a resolution of 70,000 after the accumulation of 1,000,000 ions, full-scan MS overall spectra (m/z 350–1600) in profile mode were acquired in the Orbitrap. After 50,000 ions accumulated, fragmentation by collision-induced dissociation (resolution of 17,500, normalized energy 35%) of the ten strongest peptide ions from the preview scan in the Orbitrap occurred. Top filling times were 250 ms for the whole scans, and 60 ms for the MS/MS scans. We enabled precursor ion charge state screening and rejected all unassigned charge states as well as singly, seven- and eight-charged species. We limited the dynamic exclusion list to a maximum of 500 entries with a maximum retention length of 40 s and a relative mass window of 10 ppm. To improve mass accuracy, the lock mass option was enabled. The Xcalibur software was used to acquire data (Mathieu et al., 2016).

MS data analysis

The MaxQuant software package version 1.5.1.2 was used to process, search and quantify the data collected, employing the *S. pombe* Uniprot proteome with 5142 protein annotations (Proteome ID: UP000002485), as recently described (Telekawa et al., 2018). The settings used for the MaxQuant analysis were: two miscleavages were allowed; fixed modification was carbamidomethylation on cysteine; enzyme was trypsin; variable modifications included in the analysis were methionine oxidation and protein N-terminal acetylation. For precursor ions, 7 ppm was used as mass tolerance and for fragment ions, 20 ppm was used as tolerance threshold. To obtain candid identifications with a false discovery rate (FDR) of less than 1%, every protein was considered based on the criterion that the amount of forward hits in the database was minimally 100-fold higher than the amount of reverse database hits. Each protein had a minimum of three peptides quantified. Isoforms and proteins that were indistinguishable based on their identified peptides were grouped and organized in a single line with various accession numbers.

Acknowledgements

We thank Dominique Lévesque for help with the use of MS instruments; François-Michel Boisvert, Simon Labbé, Thierry Mourer, and members of the Bachand lab for critical reading of the manuscript.

Competing interests

The authors declare no competing or financial interests.

Author contributions

Conceptualization: M.L., D.B., F.B.; Methodology: M.L., D.B., B.A., F.B.; Software: D.B.; Formal analysis: M.L., D.B., B.A., F.B.; Investigation: M.L., D.B., B.A., F.B.; Resources: M.L., D.B., B.A., F.B.; Writing - original draft: F.B.; Writing - review & editing: M.L., D.B., F.B.; Visualization: M.L., D.B., F.B.; Supervision: M.L., F.B.; Project administration: F.B.; Funding acquisition: F.B.

Funding

This work was supported by a Discovery Grant from the Natural Sciences and Engineering Research Council of Canada (NSREC) to F.B. (05482). F.B. holds a Chair from Canada Research Chairs in Quality Control of Gene Expression (230977).

Data availability

The mass spectrometry raw files have been deposited to the ProteomeXchange Consortium via the PRIDE partner repository with the dataset identifier PXD013183.

Supplementary information

Supplementary information available online at
http://jcs.biologists.org/lookup/doi/10.1242/jcs.232249.supplemental

References

Allmang, C., Petfalski, E., Podtelejnikov, A., Mann, M., Tollervey, D. and Mitchell, P. (1999). The yeast exosome and human PM-Scl are related complexes of 3′ –> 5′ exonucleases. *Genes Dev.* **13**, 2148-2158. doi:10.1101/gad.13.16.2148

Amberg, D. C. and Burke, D. J. (2016). Classical genetics with Saccharomyces cerevisiae. *Cold Spring Harb. Protoc.* **2016** doi:10.1101/pdb.top077628

Bachand, F. and Silver, P. A. (2004). PRMT3 is a ribosomal protein methyltransferase that affects the cellular levels of ribosomal subunits. *EMBO J.* **23**, 2641-2650. doi:10.1038/sj.emboj.7600265

Bähler, J., Wu, J. Q., Longtine, M. S., Shah, N. G., Mckenzie, A., III, Steever, A. B., Wach, A., Philippsen, P. and Pringle, J. R. (1998). Heterologous modules for efficient and versatile PCR-based gene targeting in Schizosaccharomyces pombe. *Yeast* **14**, 943-951. doi:10.1002/(SICI)1097-0061(199807)14:10<943::AID-YEA292>3.0.CO;2-Y

Berriz, G. F., King, O. D., Bryant, B., Sander, C. and Roth, F. P. (2003). Characterizing gene sets with FuncAssociate. *Bioinformatics* **19**, 2502-2504. doi:10.1093/bioinformatics/btg363

Branon, T. C., Bosch, J. A., Sanchez, A. D., Udeshi, N. D., Svinkina, T., Carr, S. A., Feldman, J. L., Perrimon, N. and Ting, A. Y. (2018). Efficient proximity labeling in living cells and organisms with TurboID. *Nat. Biotechnol.* **36**, 880-887. doi:10.1038/nbt.4201

Causton, H. C., Ren, B., Koh, S. S., Harbison, C. T., Kanin, E., Jennings, E. G., Lee, T. I., True, H. L., Lander, E. S. and Young, R. A. (2001). Remodeling of yeast genome expression in response to environmental changes. *Mol. Biol. Cell* **12**, 323-337. doi:10.1091/mbc.12.2.323

Chen, D., Toone, W. M., Mata, J., Lyne, R., Burns, G., Kivinen, K., Brazma, A., Jones, N. and Bahler, J. (2003). Global transcriptional responses of fission yeast to environmental stress. *Mol. Biol. Cell* **14**, 214-229. doi:10.1091/mbc.e02-08-0499

Dunham, W. H., Mullin, M. and Gingras, A.-C. (2012). Affinity-purification coupled to mass spectrometry: basic principles and strategies. *Proteomics* **12**, 1576-1590. doi:10.1002/pmic.201100523

Egan, E. D., Braun, C. R., Gygi, S. P. and Moazed, D. (2014). Post-transcriptional regulation of meiotic genes by a nuclear RNA silencing complex. *RNA* **20**, 867-881. doi:10.1261/rna.044479.114

Gasch, A. P., Spellman, P. T., Kao, C. M., Carmel-Harel, O., Eisen, M. B., Storz, G., Botstein, D. and Brown, P. O. (2000). Genomic expression programs in the response of yeast cells to environmental changes. *Mol. Biol. Cell* **11**, 4241-4257. doi:10.1091/mbc.11.12.4241

Goodacre, N., Devkota, P., Bae, E., Wuchty, S. and Uetz, P. (2018). Protein-protein interactions of human viruses. *Semin. Cell Dev. Biol*, S1084-9521(17)30499-8. doi:10.1016/j.semcdb.2018.07.018

Grenier St-Sauveur, V., Soucek, S., Corbett, A. H. and Bachand, F. (2013). Poly(A) tail-mediated gene regulation by opposing roles of Nab2 and Pab2 nuclear poly(A)-binding proteins in pre-mRNA decay. *Mol. Cell. Biol.* **33**, 4718-4731. doi:10.1128/MCB.00887-13

Hoffman, C. S., Wood, V. and Fantes, P. A. (2015). An ancient yeast for young geneticists: a primer on the schizosaccharomyces pombe model system. *Genetics* **201**, 403-423. doi:10.1534/genetics.115.181503

Hung, V., Udeshi, N. D., Lam, S. S., Loh, K. H., Cox, K. J., Pedram, K., Carr, S. A. and Ting, A. Y. (2016). Spatially resolved proteomic mapping in living cells with the engineered peroxidase APEX2. *Nat. Protoc.* **11**, 456-475. doi:10.1038/nprot.2016.018

Hwang, J. and Espenshade, P. J. (2016). Proximity-dependent biotin labelling in yeast using the engineered ascorbate peroxidase APEX2. *Biochem. J.* **473**, 2463-2469. doi:10.1042/BCJ20160106

Kim, D. I., Jensen, S. C., Noble, K. A., Kc, B., Roux, K. H., Motamedchaboki, K. and Roux, K. J. (2016). An improved smaller biotin ligase for BioID proximity labeling. *Mol. Biol. Cell* **27**, 1188-1196. doi:10.1091/mbc.E15-12-0844

Laddach, A., Ng, J. C.-F., Chung, S. S. and Fraternali, F. (2018). Genetic variants and protein-protein interactions: a multidimensional network-centric view. *Curr. Opin. Struct. Biol.* **50**, 82-90. doi:10.1016/j.sbi.2017.12.006

Lambert, J.-P., Tucholska, M., Go, C., Knight, J. D. R. and Gingras, A.-C. (2015). Proximity biotinylation and affinity purification are complementary approaches for the interactome mapping of chromatin-associated protein complexes. *J. Proteomics* **118**, 81-94. doi:10.1016/j.jprot.2014.09.011

Landry-Voyer, A.-M., Bilodeau, S., Bergeron, D., Dionne, K. L., Port, S. A., Rouleau, C., Boisvert, F. M., Kehlenbach, R. H. and Bachand, F. (2016). Human PDCD2L Is an Export Substrate of CRM1 That Associates with 40S Ribosomal Subunit Precursors. *Mol. Cell. Biol.* **36**, 3019-3032. doi:10.1128/MCB.00303-16

Lee, N. N., Chalamcharla, V. R., Reyes-Turcu, F., Mehta, S., Zofall, M., Balachandran, V., Dhakshnamoorthy, J., Taneja, N., Yamanaka, S., Zhou, M. et al. (2013). Mtr4-like protein coordinates nuclear RNA processing for heterochromatin assembly and for telomere maintenance. *Cell* **155**, 1061-1074. doi:10.1016/j.cell.2013.10.027

Lemay, J.-F., Larochelle, M., Marguerat, S., Atkinson, S., Bähler, J. and Bachand, F. (2014). The RNA exosome promotes transcription termination of backtracked RNA polymerase II. *Nat. Struct. Mol. Biol.* **21**, 919-926. doi:10.1038/nsmb.2893

Lemay, J.-F., Marguerat, S., Larochelle, M., Liu, X., Van Nues, R., Hunyadkürti, J., Hoque, M., Tian, B., Granneman, S., Bahler, J. et al. (2016). The Nrd1-like protein Seb1 coordinates cotranscriptional 3′ end processing and polyadenylation site selection. *Genes Dev.* **30**, 1558-1572. doi:10.1101/gad.280222.116

Liu, Q., Greimann, J. C. and Lima, C. D. (2006). Reconstitution, activities, and structure of the eukaryotic RNA exosome. *Cell* **127**, 1223-1237. doi:10.1016/j.cell.2006.10.037

Longtine, M. S., Mckenzie, A., III, Demarini, D. J., Shah, N. G., Wach, A., Brachat, A., Philippsen, P. and Pringle, J. R. (1998). Additional modules for versatile and economical PCR-based gene deletion and modification in Saccharomyces cerevisiae. *Yeast* **14**, 953-961. doi:10.1002/(SICI)1097-0061(199807)14:10<953::AID-YEA293>3.0.CO;2-U

Makino, D. L., Baumgartner, M. and Conti, E. (2013). Crystal structure of an RNA-bound 11-subunit eukaryotic exosome complex. *Nature* **495**, 70-75. doi:10.1038/nature11870

Mathieu, A. A., Ohl-Seguy, E., Dubois, M.-L., Jean, D., Jones, C., Boudreau, F. and Boisvert, F.-M. (2016). Subcellular proteomics analysis of different stages of colorectal cancer cell lines. *Proteomics* **16**, 3009-3018. doi:10.1002/pmic.201600314

Mellacheruvu, D., Wright, Z., Couzens, A. L., Lambert, J.-P., St-Denis, N. A., Li, T., Miteva, Y. V., Hauri, S., Sardiu, M. E., Low, T. Y. et al. (2013). The CRAPome: a contaminant repository for affinity purification-mass spectrometry data. *Nat. Methods* **10**, 730-736. doi:10.1038/nmeth.2557

Perreault, A., Gascon, S., D'amours, A., Aletta, J. M. and Bachand, F. (2009). A methyltransferase-independent function for Rmt3 in ribosomal subunit homeostasis. *J. Biol. Chem.***284**, 15026-15037. doi:10.1074/jbc.M109.004812

Rigaut, G., Shevchenko, A., Rutz, B., Wilm, M., Mann, M. and Séraphin, B. (1999). A generic protein purification method for protein complex characterization and proteome exploration. *Nat. Biotechnol.* **17**, 1030-1032. doi:10.1038/13732

Roux, K. J., Kim, D. I., Raida, M. and Burke, B. (2012). A promiscuous biotin ligase fusion protein identifies proximal and interacting proteins in mammalian cells. *J. Cell Biol.* **196**, 801-810. doi:10.1083/jcb.201112098

Roux, K. J., Kim, D. I., Burke, B. and May, D. G. (2018). BioID: A Screen for Protein-Protein Interactions. *Curr. Protoc. Protein Sci.* **91**, 19.23.1-19.23.15. doi:10.1002/cpps.51

Schwanhäusser, B., Busse, D., Li, N., Dittmar, G., Schuchhardt, J., Wolf, J., Chen, W. and Selbach, M. (2011). Global quantification of mammalian gene expression control. *Nature* **473**, 337-342. doi:10.1038/nature10098

Stolz, J. (2003). Isolation and characterization of the plasma membrane biotin transporter from Schizosaccharomyces pombe. *Yeast* **20**, 221-231. doi:10.1002/yea.959

Tasto, J. J., Carnahan, R. H., Mcdonald, W. H. and Gould, K. L. (2001). Vectors and gene targeting modules for tandem affinity purification in Schizosaccharomyces pombe. *Yeast* **18**, 657-662. doi:10.1002/yea.713

Telekawa, C., Boisvert, F.-M. and Bachand, F. (2018). Proteomic profiling and functional characterization of post-translational modifications of the fission yeast RNA exosome. *Nucleic Acids Res.* **46**, 11169-11183. doi:10.1093/nar/gky915

Tong, L. (2013). Structure and function of biotin-dependent carboxylases. *Cell. Mol. Life Sci.* **70**, 863-891. doi:10.1007/s00018-012-1096-0

Van Driessche, B., Tafforeau, L., Hentges, P., Carr, A. M. and Vandenhaute, J. (2005). Additional vectors for PCR-based gene tagging in Saccharomyces cerevisiae and Schizosaccharomyces pombe using nourseothricin resistance. *Yeast* **22**, 1061-1068. doi:10.1002/yea.1293

Zhou, Y., Zhu, J., Schermann, G., Ohle, C., Bendrin, K., Sugioka-Sugiyama, R., Sugiyama, T. and Fischer, T. (2015). The fission yeast MTREC complex targets CUTs and unspliced pre-mRNAs to the nuclear exosome. *Nat. Commun.* **6**, 7050. doi:10.1038/ncomms8050

Zinder, J. C. and Lima, C. D. (2017). Targeting RNA for processing or destruction by the eukaryotic RNA exosome and its cofactors. *Genes Dev.* **31**, 88-100. doi:10.1101/gad.294769.116